BIOCHEMISTRY
including biophysical chemistry & molecular biology

Article

pubs.acs.org/biochemistry

Histone Peptide Recognition by KDM5B-PHD1: A Case Study

Suvobrata Chakravarty,*[,†] Francisca Essel,[†] Tao Lin, and Stad Zeigler

Department of Chemistry & Biochemistry, South Dakota State University, Box-2202, SAV367, Brookings, South Dakota 57007, United States

Supporting Information

ABSTRACT: A detailed understanding of the energetic contributions to histone peptide recognition would be valuable for a better understanding of chromatin anchoring mechanisms and histone diagnostic design. Here, we probed the energetic contributions to recognize the same unmodified histone H3 by three different plant homeodomain (PHD) H3K4me0 *readers*: hKDM5B-PHD1 (first PHD finger of hKDM5B), hBAZ2A-PHD, and hAIRE-PHD1. The energetic contributions of residues differ significantly from one complex to the next. For example, H3K4A substitution completely aborts the formation of the hAIRE−histone peptide complex, while it has only a small destabilizing effect on binding of the other readers, even though H3K4 methylation disrupts all three complexes. Packing density suggests that methylation of more tightly packed Lys/Arg residues can disrupt binding, even if the energetic contribution is small. The binding behavior of hKDM5B-PHD1 and hBAZ2A-PHD is similar, and like PHD H3R2 *readers*, both possess a pair of Asp residues in the treble clef for interaction with H3R2. PHD subtype sequences, especially the tandem PHD−PHD fingers, show enrichment in the treble clef Asp residues, suggesting that it is a subtype-specific property. These Asp residues make significant energetic contributions to the formation of the hKDM5B−histone peptide complex, suggesting that there are interactions in addition to those reported in the recent NMR structure. However, the presence of the treble clef Asp in PHD sequences may not always be sufficient for histone peptide binding. This study showcases *reader*−histone peptide interactions in the context of residue conservation, energetic contributions, interfacial packing, and sequence-based *reader* subtype predictability.

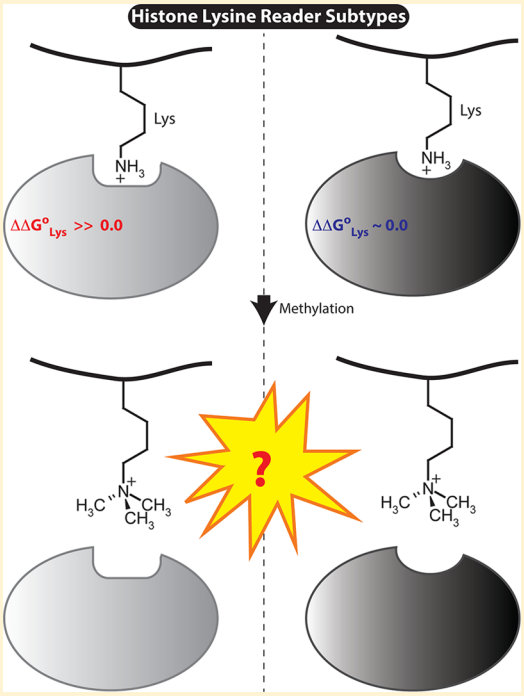

Histone tails are critical information-retrieval hubs, and several proteins bind them to orchestrate chromatin signaling pathways, which collectively regulate chromatin structure and thereby exert ultimate control over all the diverse biological outcomes associated with chromatin.[1] The recognition of disordered peptide segments of histones is a crucial component of these pathways. Histone peptide segments, with or without site-specific post-translational modifications (PTMs), provide the binding surface for regulatory protein complexes to anchor onto chromatin. In general, peptide-mediated signaling operates with a three-part toolbox,[2−4] consisting of modular protein domain families of (a) enzymes that catalyze the addition of site-specific PTMs, called marks, (b) peptide-anchoring modules that bind peptides with or without the marks,[5−7] and (c) enzymes that catalyze the removal of these marks. In other words, *writers* (methylases and acetylases) *write* specific marks, *readers* (peptide binding domains) interpret the marks, and *erasers* (demethylases and deacetylases) erase the marks.[3,4] Anchoring of unmodified histones (histone peptides bearing no marks) by *readers* is a crucial component of chromatin regulation, as introduction of marks at these sites can disrupt such anchoring and thereby regulate information flow. However, compared with the number of reported *readers* of histone site-specific PTMs, there are fewer reports on the readout of unmodified histones.[5−7] Hence, to better understand the mechanism of readout of unmodified histones, we focused on one specific *reader*, the first PHD finger of human KDM5B (hKDM5B-PHD1), which specifically binds the unmodified histone H3 N-terminal peptide.[8,9] This interaction probably contributes to the variety of crucial roles, such as regulating key developmental and lineage specification genes,[10] genome stability,[11] embryonic stem cell renewal,[12] and cancer growth[13,14] that KDM5B plays in human chromatin signaling.

hKDM5B, the histone H3 Lys4-specific demethylase,[15,16] possesses three PHD finger modules (Figure 1C), and the N-terminal (hKDM5B-PHD1) and the C-terminal (hKDM5B-

Received: June 4, 2015
Revised: August 6, 2015
Published: August 12, 2015

DOI: 10.1021/acs.biochem.5b00617
Biochemistry 2015, 54, 5766−5780

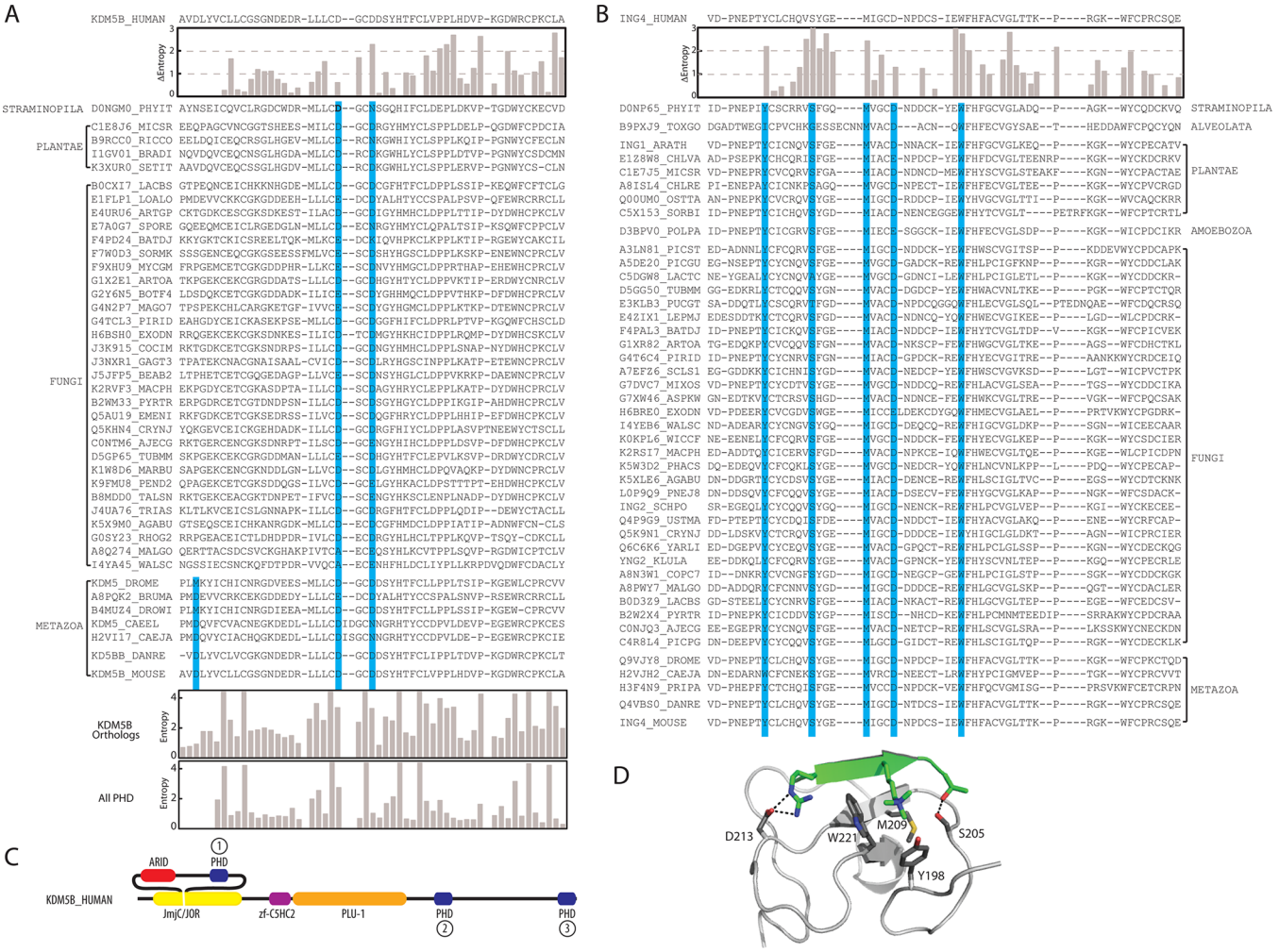

Figure 1. Human KDM5B and ING4 PHD fingers: (A) Alignment of hKDM5B-PHD1 orthologous sequences with their taxonomic groups (left). The bottom two histograms represent Entropy (see Methods) as a function of the sequence positions (hKDM5B-PHD1 orthologues and the PHD finger domain, respectively, as upper and lower histograms). The top histogram represents ΔEntropy, i.e., the numerical difference between the bottom two corresponding histogram-bars for each position. Asp residues discussed in the text are highlighted in cyan. (B) Alignment of hING4 orthologues (bottom) with ΔEntropy (top). Side-chains of hING4 residues making contact with the peptide are in cyan in the alignment (bottom). KDM5B_DANRE, KDM5B_MOUSE are retained here (but not in the calculations) only to represent metazoan subgroups. (C) Schematic representation of full-length hKDM5B with the constituent domains. The ARID and the PHD1 domains are inserted into the JmjC/JOR domain of hKDM5B. (D) Structure of hING4-PHD in complex with the H3K4me3 peptide. Side chains of hING4 residues making contacts with the peptide are in sticks.

PHD3) PHD fingers have recently been shown to, respectively, *read* H3K4me0 and H3K4me3 marks.[8] The NMR structure of hKDM5B-PHD1 in complex with the histone H3 N-terminal peptide has also been reported very recently, which elegantly captures the key *reader*−histone peptide interfacial interactions.[9] Our results, however, show that there are additional key *reader*−histone peptide inter-residue interactions for hKDM5B-PHD1. Hence, to complement the recent structural study on hKDM5B-PHD1,[9] we provided the energetic contributions of interfacial residues in the interaction between hKDM5B-PHD1 and unmodified histone H3.

With the recent elegant report on successfully utilizing histone peptide binding domains in diagnostic applications,[17,18] the demand for redesigning these *reader* modules for targeting specific histone sites is expected to rise. In general, dissection of the energetic contribution of residues at the binding interface is very informative for the purpose of protein design.[19] As a first step, here we compared the energetic contributions in the interactions of the same histone peptide with different *readers*, such as hKDM5B-PHD1, hBAZ2A-PHD, and hAIRE-PHD1, to better understand the similarities and differences in the recognition strategies adopted by *readers* of the same fold. In this study, we also utilized an interfacial packing measure to better understand the binding behavior of different *readers*, especially on the effect of different PTMs. Interfacial packing is crucial for molecular interactions, and a better understanding of the role of packing in the context of PTMs will be very useful for design applications.

Residue side chains at the peptide binding site of proteins generally tend to show small conformational changes upon peptide binding:[20] specifically, a peptide tends to bind like *lock and key* onto preformed binding surfaces.[21] This adaptation likely minimizes the entropic penalty associated with the folding transition of the peptide upon binding.[20] This adaptation can be useful in predicting a domain family member's ability to bind specific peptide sequences, as an extensive conformational search may not be necessary. Because of the lack of conformational changes, the presence of the

DOI: 10.1021/acs.biochem.5b00617
Biochemistry 2015, 54, 5766−5780

peptide-anchoring residues at specific positions (i.e., the binding site amino acid composition) may even guide the prediction of a domain family member's binding preferences based on sequence information alone. For example, PDZ domain peptide-binding subtypes are predictable based on PDZ and peptide sequence information[22] without the need for structural/conformational information. Like, PDZ domains, PHD fingers bind terminal peptides by β augmentation,[23] and this similarity encouraged us to examine the predictability of the binding behavior of PHD family members based on sequence information. Predictability of the binding behavior for the diverse sequences of a superfamily, such as the PHD finger family, can be challenging. In this study, we tested the effect on binding predictability of a specific sequence feature of hKDM5B-PHD1 and hBAZ2A-PHD. As PHD fingers are widespread in all eukaryotes, sequence-based subtype prediction would be beneficial for functional annotation. Overall, we provide a case-specific study of reader−histone peptide interactions in the context of residue conservation, residue energetic contributions, interfacial packing, and sequence-based predictability.

METHODS

Protein Expression, Purification, and Site Directed Mutagenesis. The recombinant GST fusion hKDM5B-PHD1 (residues 305−366 of UniProt ID Q9UGL1/KDM5B_Human), hKDM5D-PHD1 (residues 310−372 of UniProt ID Q9BY66/KDM5D_Human), hRSF1-PHD (residues 888−949 of UniProt ID Q96T23/RSF1_Human), and hAIRE-PHD1 domains were purified as described in Chakravarty et al.[24] Briefly, *E. coli* BL21 (DE3) cells expressing these proteins from the pGEX-4T3 vector were induced at OD_{600} = 0.6−1.0 with 1 mM IPTG grown overnight at 16 °C. The fusion proteins were isolated using GST affinity chromatography (Pierce glutathione agarose, Thermo scientific). GST tag was eliminated by overnight human alpha thrombin (Haematologic Technologies) digestion at 4 °C. The proteins were then purified to homogeneity by gel filtration using a HiLoad 26/600 superdex column using FPLC. The purity was confirmed by SDS−PAGE. Mutants (D308A, D328A, D331A) of hKDM5B-PHD1 were purified similarly. Site directed mutagenesis was carried using QuikChange Lightning Site-Directed Mutagenesis Kit (Agilent Technologies). The BAZ2A-PHD finger (residues 1673−1728 UniProt ID Q9UIF9/BAZ2A_Human) was cloned into a pETite N-His SUMO Kan expression vector and purified using a His-tag affinity column following the same expression and purification conditions as those described above.

Isothermal Titration Calorimetry (ITC). The peptides and protein for ITC were both prepared in the same buffer (25 mM phosphate and 250 mM sodium chloride at pH 7.6). The thermodynamics of binding between hKDM5B-PHD1 and the synthetic peptides were studied using MicroCal ITC200 (GE Healthcare) with protein (0.1−0.15 mM) and peptide (10-fold higher), respectively, loaded in the cell and syringe at 25 °C. Twenty 2 μL-injections with a 3 min injection-interval, with a syringe stirring speed of 1000 rpm were used for the titrations. ΔG° of peptide binding at 25 °C was computed as $-RT\ln(K_a)$ where R, T and K_a are, respectively, the gas constant, temperature, and association constant. $\Delta\Delta G^\circ$ for a residue's energetic contribution is estimated as $\Delta\Delta G^\circ = \Delta G^\circ_{mutant} - \Delta G^\circ_{wild\text{-}type}$. All titrations were carried out in identical conditions of buffer and temperature. In the case of many of the mutants, we do not observe binding (i.e., negligible amount of observed heats), and data fitting is unreliable to the observed enthalpy. In such cases, we assume that $\Delta\Delta G^\circ$ ($\gg$ 1.5 kcal·mol^{-1}) is large. Ninety-eight percent pure (confirmed with mass spectrometry) synthetic peptides, all possessing a C-terminal Trp residue, were obtained from GenScript. Trp residue of the PHD finger, as well as all of the peptides, was used for accurately estimating peptide/protein concentrations using the computed molar extinction coefficient.[25]

Colorimetric Peptide-Binding Assay. In addition to ITC, we also performed a colorimetric peptide-binding assay (Figure 6) in which quantification of the color provided a relative estimate of peptide binding affinity. Interactions of KDM5B-PHD1 (Figure 6B) and AIRE-PHD1 with histone peptide mutants fused to mCitrine were tested using this approach. FPLC purified GST-hKDM5B-PHD1 (0.5 mL) (0.05 mM−0.1 mM) was incubated with 0.1 mL of Pierce glutathione agarose (Thermo Scientific) for 2 h at 4 °C to allow the GST-fusion protein to bind to the beads. Beads were then washed 3−4 times with a total of 4 mL of phosphate buffer (25 mM phosphate and 250 mM NaCl at pH 7.6) to remove the excess unbound protein. Following the wash, 0.5 mL of FPLC purified wild type or mutant histone H3-mCitrine fusion proteins (0.5 mM−1 mM each) were then incubated with the GST-fusion protein-bound beads overnight at 4 °C. The beads were washed 3−4 times to remove unbound fluorescent proteins to visually check for the retained yellow color. Spectroscopic estimate of the color retained in the beads was obtained using a Synergy H1 BioTek fluorescent microplate reader by monitoring fluorescence at 515 (±5) nm with the beads placed in a 96-well plate. Each data point in Figure 6C is an average of four independent measurements.

Histone H3 residues 1−15 were fused to the N-terminus of mCitrine. The H3-1-15-mCitrine-His-tag fusion was inserted into pET28A using the *Nco*I and *Xho*I restriction sites so that H3 is placed immediately following the ATG start codon. This allowed H3 to be expressed with a free amino terminal (NH_2-ARTKQ-) upon removal of the terminal methionine residue. The free amino terminal (NH_2-ARTKQ-) is required for binding to PHD fingers. The removal of the terminal methionine in the H3 residues 1-15 construct was confirmed using mass spectrometry. Single site histone H3 point mutants (A1G, R2A, T3A, K4A, Q5A, T6A, and R8A) were created using the above mutagenesis kit. These *colored* proteins were then purified using His-tag affinity and gel filtration chromatography following the above expression and purification conditions. The His-tag in these constructs can be removed by thrombin proteolysis.

Alignment of Orthologues and Residue Entropy. UniProt[26,27] IDs of orthologues of human proteins containing PHD fingers were manually downloaded from the InParanoid database,[28] and the sequences of these orthologues were then obtained from UniProt. We obtained InParanoid[28] orthologues with default parameters. The orthologous sequences were aligned using MUSCLE,[29] and the segment of the alignment corresponding to the domain of interest in the human sequence was selected for further analysis. Redundant sequences at 75% sequence identity were then eliminated to compute entropy at each position of the alignment. Entropy for the ith position was computed as, Entropy = $4.39 - \Sigma(p_j) \times (\log_2(p_j))$, where p_j is the probability of the jth amino acid at the ith position/column, and 4.39 is the value of maximum entropy. Reference PFAM[30] alignments were treated similarly, i.e., the removal of redundancy followed by entropy calculation. ΔEntropy for

DOI: 10.1021/acs.biochem.5b00617
Biochemistry 2015, 54, 5766−5780

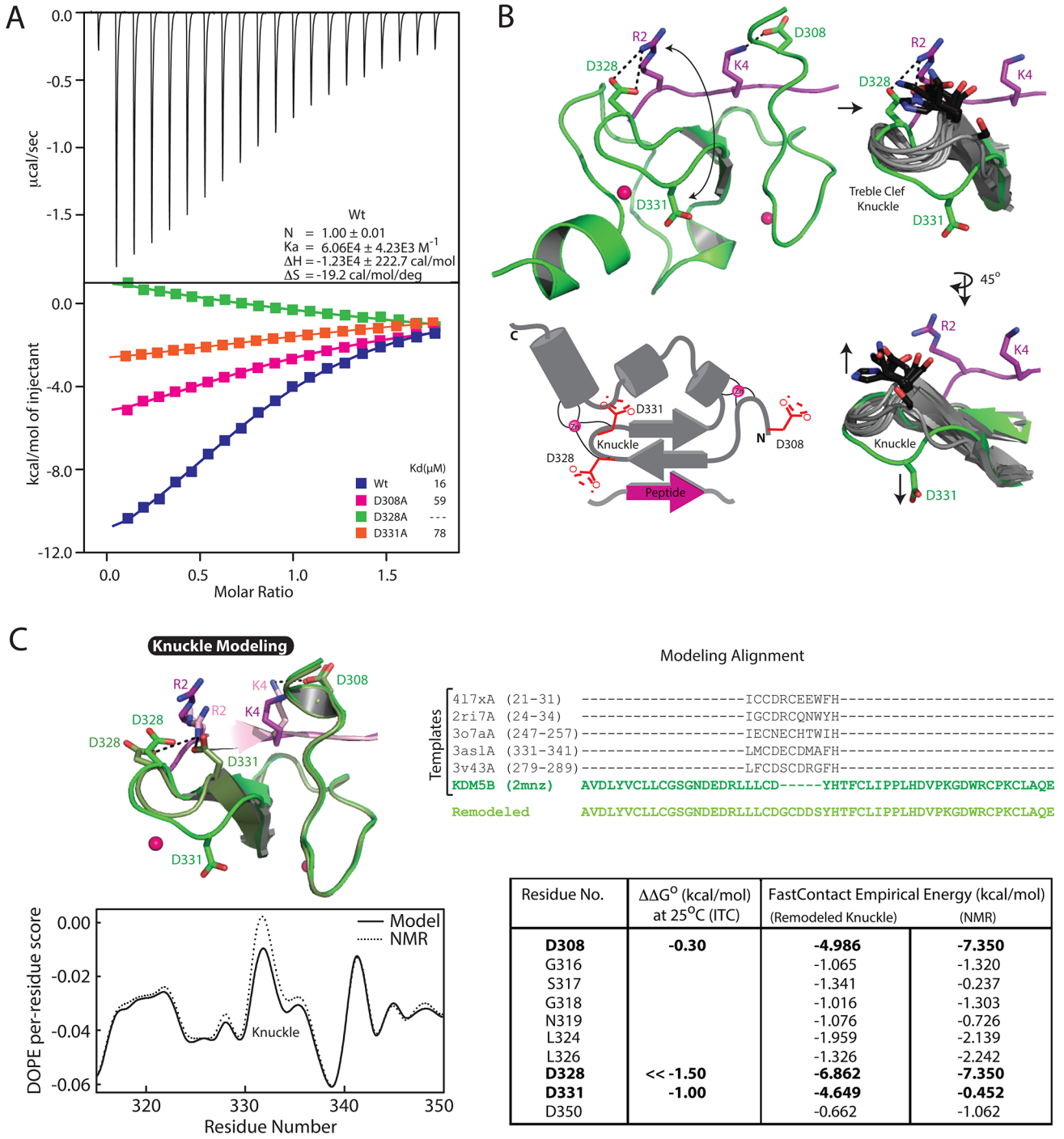

Residue No.	ΔΔG° (kcal/mol) at 25°C (ITC)	FastContact Empirical Energy (kcal/mol) (Remodeled Knuckle)	(NMR)
D308	**-0.30**	**-4.986**	**-7.350**
G316		-1.065	-1.320
S317		-1.341	-0.237
G318		-1.016	-1.303
N319		-1.076	-0.726
L324		-1.959	-2.139
L326		-1.326	-2.242
D328	**<< -1.50**	**-6.862**	**-7.350**
D331	**-1.00**	**-4.649**	**-0.452**
D350		-0.662	-1.062

Figure 2. Asp residues and the PHD knuckle: (A) ITC binding studies between histone H3 unmodified N-terminal peptide and wild type, mutants of KDM5B-PHD1. A representative isothermal calorimetric titration (top) of the H3-1-9 peptide (syringe) into protein (cell) is shown for the wild type protein, while exothermic heats (bottom) exchanged per mol of injectant as a function of the molar ratio of peptide to protein is overlaid for all titrations for convenience. (B) The orientation of the treble clef knuckle Asp331 (green sticks) in the KDM5B-PHD1 NMR structure (*2mnz*) is different from that seen for residues at that position in the knuckles of other PHD fingers (black sticks). This orientation places Asp331 distant from the peptide (purple) Arg2 residue. The PHD topology cartoon (bottom left) represents the symbolic positions of the Asp residues (red). (C) (Top Left) Remodeled knuckle (split pea) reorients Asp331 leaving the rest of the chain structurally unaltered (split pea and green); (top right) the modeling alignment with PDB IDs and residue numbers of the templates; (bottom left), DOPE per-residue score for the knuckle; (bottom right), FastContact empirical energies and $\Delta\Delta G^{o}$ estimated from ITC.

each position of a particular PHD-finger was obtained by subtracting the PFAM reference entropy for the position (see Figure 1A). CD-Hit[31] was used to eliminate redundant sequences. A single sequence for the mammalian orthologue of KDM5B-PHD1 (Figure 1A) means that all mammalian sequences are nearly identical and that elimination of redundant sequences at 75% sequence identity leaves one representative sequence.

Homology Modeling and Empirical Energy Calculations. Homology modeling of the hKDM5B-PHD1 Zn-

DOI: 10.1021/acs.biochem.5b00617
Biochemistry 2015, 54, 5766−5780

anchoring treble clef was carried using MODELER 9v11[32] based on the alignment (see Figure 2C, top right). The coordinates of PHD-fingers with resolution better than 2.0 Å and having an xCxxCx-type treble clef were used as a template to remodel the treble clef while the remaining part of template was inherited from the coordinate file *2mnz* after deleting the coordinates of the atoms of the KDM5B-PHD1 knuckle. The modeling included both the *reader* and the peptide though the Figure 2C alignment does not show the peptide. DOPE (Discrete Optimized Protein Energy)[33] per-residue score was used to evaluate the model quality with respect to the experimental structure, and inter-residue empirical interaction energies were obtained using the FastContact algorithm.[34,35] DOPE is an atomic distance dependent statistical potential from a sample of native structures representing an improved reference state of noninteracting atoms in a homogeneous sphere with the radius dependent on a sample native structure, and the energy scale is independent of adjustable parameters.[33] DOPE was used for its superior performance in evaluating homology models,[33] and its implementation within the MODELER package for usage convenience. FastContact provides a rapid estimate of contact and binding free energies for protein−protein complex structures, and the algorithm is based on a statistically determined desolvation contact potential and Coulomb electrostatics with a distance-dependent dielectric constant.[34] FastContact provides residue contact free energies that highlight the interaction hotspots.[34] We used the FastContact Web server[35] by uploading the coordinate files of the *reader* and that of the peptide.

PHD Subtype and Tandem PHD−PHD. We used the 75% nonredundant PFAM-aligned[30] PHD family sequences for all the subtype specific calculations. CD-Hit[31] was used to eliminate redundant sequences. Residue type frequency at a position in the alignment is computed as the probability of the *j*th residue type at the *i*th position. The nonredundant alignments are then split to two groups: PHD_W and PHD_nW based on the presence and absence of aromatic residues at the PHD beta strand *W-position*. The probability of the *j*th residue type at the *i*th position in the PHD_W and PHD_nW groups are conditional probabilities (see text).

The default PFAM PHD-finger domain's residue boundary was used to select tandem PHD−PHD sequences in the following manner. UniProt ids having two or more PHD fingers in the PFAM alignment were selected first. Then, the number of residues (*nb*) between two adjacent PHD fingers was noted. For example, A5PLL3_HUMAN has two PFAM PHD fingers (PHD1 208−265 and PHD2 264−313) and $nb = -1$ in this examples. We select sequences where $nb = -1$, 0, 1, 2, and 3. For a majority of tandem PHD−PHD, *nb* is equal to −1. All UniProt IDs with multiple PHD fingers and having *nb* between −1 and 3 were aligned after eliminating the redundant sequence at 75% sequence identity to create the Figure 5B alignment.

Packing Density. We used the Voronoia program[36] to compute packing density of atoms. Voronoia implements the Voronoi cell method[37] to allocate space between every pair of neighboring points/atoms. The Voronoi cell method uses hyperbolic surfaces instead of planes (in the original Voronoi method) to allocate space. This approach overcomes the difficulty of allocating space to surface exposed atoms.[37] The Voronoia program reports packing density (PD) of an atom as the ratio, $PD = V_{vdW}/(V_{vdW} + V_{se})$, where V_{vdW} is the volume inside the van der Waals sphere of an atom, and V_{se} is the remaining solvent excluded volume assigned to each atom.[36] For PD of a set of atoms, we average the PDs of the set of atoms of interest. Only high-resolution structures (resolution ≤2.0 Å) were considered for packing calculations. Atom depth[38] is computed here as the distance from the nearest surface atom (atoms with nonzero surface area).

Peptide Hot Spot Propensity. Using the Pepx[39] high resolution peptide−protein complex structural data set, we carried out peptide hot spot propensity calculations following the procedure of London et al.[20] Briefly, Rosetta Alanine scanning mutagenesis[19] was used to estimate the energetic contribution of peptide residues in the selected peptide−protein complexes. Peptide residues with $\Delta\Delta G$ of 1 kcal/mol or more were considered hot spots. One hundred forty peptide−protein complexes, where the peptide had at least one Arg residue, were selected for calculations. Similarly, 130 peptide−protein complexes, where the peptide had at least one Lys residue, were selected. The number of complexes used here is comparable to the number (∼100 complexes) used in the original London et al.[20] calculations. The frequency of occurrence (Fr_e) of peptide amino acids when making large energetic contributions toward overall binding ($\Delta\Delta G \geq 1$ kcal/mol) and the frequency of occurrence peptide amino acids at the binding site (Fr_b) are used to compute the propensity ratio (Fr_e/Fr_b). Peptide residue with the propensity ratio (Fr_e/Fr_b) > 1.0 is considered a hot spot. The conclusion does not change when imposing a $\Delta\Delta G$ cutoff of 2 kcal/mol.

KDM5D-PHD1 and Peptide Swapping. Author: The NMR structure of KDM5D-PHD1 (pdb 2e6r), available from the Structural Genomics Consortium, was used for this analysis. The KDM5D-PHD1 structure is compared with other PHD structures to understand why the histone peptide cannot place itself within the canonical binding site of KDM5D-PHD1. We selected PHD−peptide complexes that deviate by <1.5 Å from the KDM5D-PHD1 structure and placed the corresponding peptide's backbone atoms within the KDM5B-PHD1 binding site without any peptide conformational adjustments. This is achieved by structural superposition of a PHD−peptide complex onto KDM5D-PHD1. The transformed coordinates of the peptide are then appended to the KDM5D-PHD1 coordinate file. HBPLUS[40] is used to examine the peptide backbone hydrogen bond lengths when the peptide is placed artificially within the KDM5B-PHD1 binding site. As a positive control, this experiment is repeated with a set of PHD finger that bind peptides. For example, the peptide of BHC80-PHD is placed onto the binding site of NSD3-PHD without peptide conformation adjustments after superposing BHC80-PHD onto NSD3-PHD. Here, we refer to this as peptide swapping. Hydrogen bond lengths in the swapped complexes were then examined. The distribution of the hydrogen bond lengths is then compared (Figure S7B, bottom). All of the 20 ensemble structures of KDM5D-PHD1 (pdb 2e6r) are used in this experiment.

RESULTS AND DISCUSSION

Domain and Residue Conservation of KDM5B-PHD1. The majority of structural mechanisms elucidating the recognition of cognate peptides by PHD finger modules has come predominantly from human proteins.[41] Mapping the orthologues of these PHD finger-containing human proteins from completely sequenced eukaryotes onto the branches of the eukaryote tree of life[42] is valuable for understanding the origins of these proteins. Such a mapping (Figure S1A) shows

DOI: 10.1021/acs.biochem.5b00617
Biochemistry 2015, 54, 5766−5780

that KDM5B, ING4, CHD4, UHRF1, and a few other proteins are present in the major branches of the eukaryote tree of life, while AIRE, DNMT3L, DNMT3A, DPF3, and others are present exclusively in the metazoan branch. This suggests that, among PHD-containing human proteins, KDM5B, ING4, CHD4, and UHRF1 are likely to be early "inventions," and that mapping the sequences of the PHD finger modules of these proteins onto their respective structures would highlight the evolutionary history of peptide-anchoring residues. One also notes that, unlike the other *reader* proteins, KDM5B and ING4 orthologues are present in several fungal species (Figures 1 and S1A). Upon elimination of redundant sequences at 75% sequence identity, we found that sequences of KDM5B-PHD1 and ING4-PHD orthologues are more diverse (Figure 1) compared with orthologues of CHD4 and UHRF1 PHD fingers (Figure S1B), and this is due to sequence diversification in the fungal lineage (see Methods).

Even though there are diverse ING4-PHD orthologous sequences, it is interesting to note that human ING4 residues making side-chain contacts with the histone peptide are among the most highly conserved, as reflected in the large ΔEntropy values (Figure 1B,D). A large value of ΔEntropy (see Methods) at a position indicates a preference among the orthologues for a particular residue at that position compared with the PHD family background frequency of this residue at the same position. A large ΔEntropy value (≥2.0) for peptide-interacting positions in ING4 encouraged us to investigate the contribution of KDM5B-PHD1 residues with large ΔEntropy. For KDM5B-PHD1, Asp308 was highlighted for anchoring histone H3 Lys4 in the recent structural study on KDM5B-PHD1 in complex with H3.[9] Interestingly, Asp308 is observed only in the metazoan lineage, while Asp328 and Asp331 are present in almost all of the diverse orthologous sequences (Figure 1A). Asp331 (which is in the vicinity of the binding site), like the ING4 example, shows a large ΔEntropy value, suggesting that it might play a role in peptide recognition. However, the previous structural study on KDM5B-PHD1[9] reported negligible chemical shifts for the backbone amide ^{1}H and ^{15}N atoms of Asp331 upon peptide binding. Moreover, Asp331, in the NMR structure, is far from any of the histone peptide residues (Figure 2B). Therefore, we wanted to compare the energetic contribution of Asp331 to that of Asp308 and Asp328, if indeed Asp331 had any contribution comparable to that of the two Asp residues implicated in anchoring the histone peptide in the previous structural study.[9]

Energetic Contributions of Asp Residues toward Peptide Binding. These Asp residues were individually replaced by Ala, and the change in the binding free energy or the affinity for the synthetic histone H3 peptide for the mutants was noted (Figure 2A). Isothermal titration calorimetry (ITC) was used to estimate the peptide binding affinity (K_d) of 16 μM for wild type and 59 μM and 78 μM, respectively, for the D308A and D331A mutants (Figure 2A). This result suggests that Asp331 indeed makes an energetic contribution to peptide binding. The contribution of Asp331 ($\Delta\Delta G \sim 1.0$ kcal/mol) is larger than that of Asp308 (~0.7 kcal/mol), but D328A did not show any detectable binding: specifically, D328 has a very large energetic contribution, and replacement of D328 aborts peptide binding. In examining the NMR structure, one notes that the orientation of the Asp331 side chain in the treble clef of KDM5B-PHD1 is very different from what is usually observed in xCxxCx-type knuckles of PHD fingers (Figure 2B). This places Asp331 in the recent structure distant from the histone peptide Arg2 residue. In the structures of UHRF1 and KAT6A PHD fingers, *readers* of H3R2,[43,44] the histone H3 peptide Arg2 residue makes salt bridges with the Asp residues positioned similarly in the knuckle (Figure S3). Hence, we anticipated that for KDM5B-PHD1, the Asp331 side chain carboxylate would interact with the histone peptide Arg2 residues. The treble clef in the NMR structure was remodeled using homology modeling to reorient the Asp331 using the xCxxCx-type PHD treble clefs as templates (Figure 2C) to place the Asp331 carboxylate proximal to the histone peptide Arg2 guanidinium group, while leaving the rest of the polypeptide chain unaltered in the modeling experiment. Using the FastContact algorithm,[34] empirical energy contributions of residues at the binding interface were computed to show that the contributions of Asp residues in the remodeled structure are in better agreement with the experimentally observed contributions than in the NMR structure (Figure 2C). In other words, the residue contribution, $\Delta\Delta G$, in the decreasing order D328 > D331 > D308 observed experimentally agrees better with the order using the FastContact energies for the remodeled knuckle. The discrete optimized protein energy (DOPE) per-residue energy score[33] also shows that the remodeled treble clef has lower energy than the corresponding NMR structure (Figure 2C). However, the knuckles of the templates showed even lower DOPE per-residue energy scores (~0.44 on average), suggesting that further refinement may be necessary. Recent elegant work on the refinement of NMR structures using the ROSETTA suite shows quality improvements comparable to that of X-ray structures,[45,46] and KDM5B-PHD1 may require similar refinement. In short, conservation of residues among diverse orthologues can be useful for checking a residue's contribution and its structural implications. Like the UHRF1 and KAT6A PHD fingers, KDM5B-PHD1 may similarly resemble Arg2 anchoring by the paired Asp residues of the knuckle (Figure S3). This resemblance also suggests that ancient versions of KDM5B-PHD1 probably had the capability of interacting with H3R2 through its dicarboxylates, while it acquired the capability to anchor H3 Lys4 in the metazoan lineage. Detailed experiments would, however, be needed to demonstrate the ancient peptide-binding behavior. An earlier report on hKDM5B demethylase had also shown that deletion of the PHD1 compromises KDM5B demethylase activity.[16] For the highly conserved nature of peptide anchoring residues of PHD1, it is also tempting to speculate that PHD1 is likely to be indispensible for the demethylase activity of ancient KDM5B.

In the recently reported 1.9-Å X-ray structure of BAZ2A-PHD in complex with the unmodified histone H3 N-terminal peptide, one does not observe the typical salt bridge needed for anchoring H3 Lys4.[47] This behavior is atypical of all the known *readers* of H3K4, where at least one salt bridge engages the peptide H3 Lys4 residue (Figure S3). In the BAZ2A-PHD H3 peptide complex, the H3K4 side chain is exclusively hydrogen bonded to PHD finger backbone residues.[47] The absence of the salt bridge is due to the absence of the Asp/Glu residue(s) N-terminal to the first Cys, which typically engage the H3K4 residue by a salt bridge in all the known PHD finger H3K4 *readers* (Figure S3). Like BAZ2A, BAZ2B-PHD also lacks the salt-bridging Asp/Glu yet binds the unmodified histone H3 N-terminal peptide.[47] It is, however, interesting to note that both BAZ2A- and BAZ2B-PHD contain the pair of Asp residues (D1695 and D1698 in BAZ2A) in the treble clef knuckle, similar to the pair of D328 and D331 residues in KDM5B-PHD1 (Figure S3), discussed above, for having energetic

DOI: 10.1021/acs.biochem.5b00617
Biochemistry 2015, 54, 5766−5780

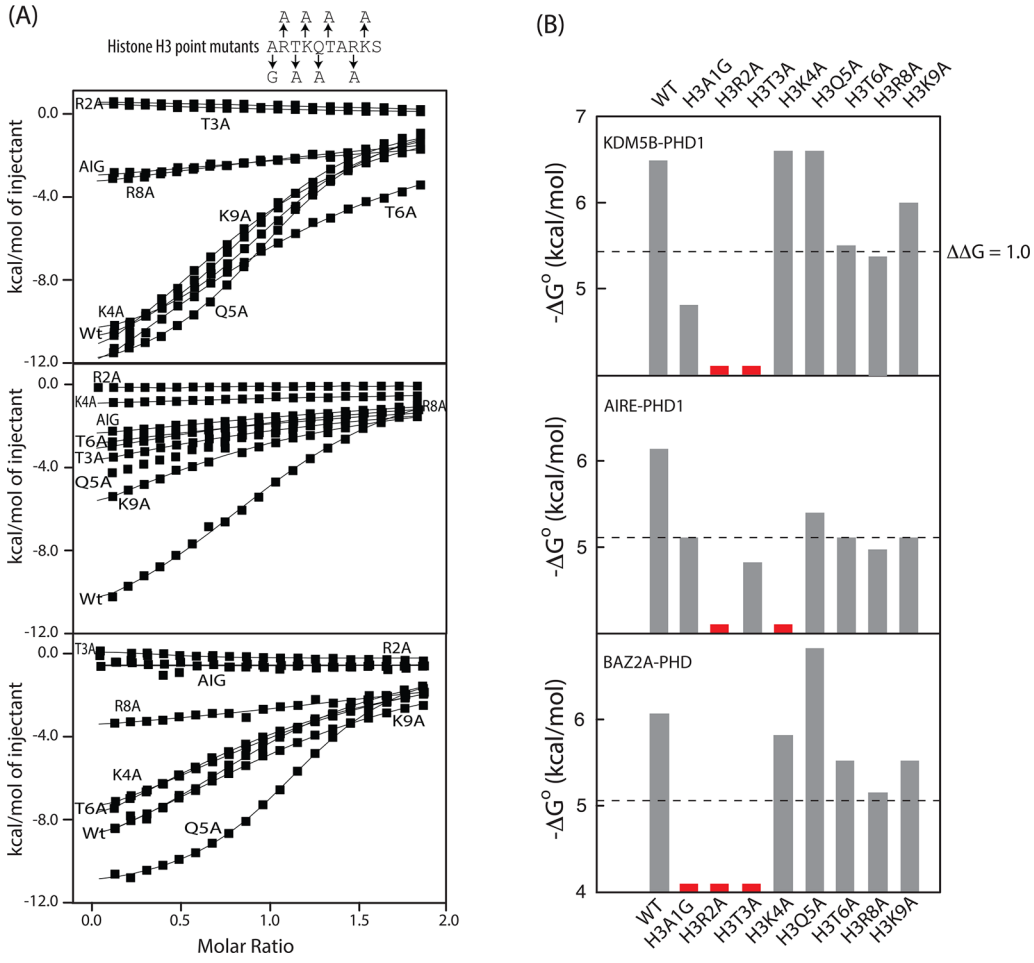

Figure 3. Peptide residue contributions: (A) ITC titration profiles of hKDM5B-PHD1 (top), hAIRE-PHD1 (middle) and hBAZ2A-PHD (bottom) with histone H3 wild type and mutant peptides. (B) ΔG° of the forward binding reaction is shown for the three *readers*. For convenience $-\Delta G^{\circ}$ is shown. Residues that contribute more than 1 kcal/mol of free energy are below the dotted line. Red bars are for positions where binding was not detected in ITC experiments.

contributions toward peptide binding. In other words, PHD fingers lacking the exclusive salt bridge for the H3K4 residue can also bind the unmodified N-terminal H3. Hence, the smaller destabilization of the KDM5B-PHD1-H3 peptide complex upon D308A mutation may not rule out the additional possibility of engaging the H3 Lys4 side chain with KDM5B backbone hydrogen bonds similar to that observed in the BAZ2A complex.

Energetic Contributions of Peptide Residues. Having observed differences in the energetic contributions of the *reader* residues with those reported in the previous structural study, we then similarly examined the contributions of the histone peptide residues using ITC. The energetic contributions of these residues in binding to KDM5B-PHD1 are also compared with those of BAZ2A-PHD and AIRE-PHD1 to see the similarities and differences between *readers*, as they all bind the same region of histone H3. Though the structures of BAZ2A-PHD and AIRE-PHD1 are available, the energetic contributions of the histone peptide residues have not been reported. Contributions of histone peptide residues are most commonly examined with respect to post-translational modifications, and determining the energetic contribution of residues by replacing them with Ala is valuable for comparing the binding strategy adopted by different *readers*. Hence, all the positions of histone H3 residues 2−9 in the synthetic peptides were replaced with Ala, while H3A1 was replaced with Gly (Figure 3A). For KDM5B-PHD1, we observed that selected histone residues make large energetic contributions to the overall binding energetics (Figure 3A,B). For KDM5B-PHD1 and BAZ2A-PHD, we observed a negligible amount of heat of binding for replacements of H3R2 and H3T3; in other words, we did not observe any binding for mutants at these positions. The energetic contributions of these positions are expected to be more than ∼1.5 kcal/mol (Figure 3B). The rest of the residues have energetic contributions between 1 and 0 kcal/mol (Figure 3B). The observed energetic contributions are in agreement with those reported in the recent structural study.[9] However, in addition to these residues, we observed that Arg8 also makes a contribution of ∼1.0 kcal/mol. It is interesting to note that for BAZ2A-PHD, the energetic contributions of the histone peptide residues are very similar to that of KDM5B-PHD1; specifically, H3A1, H3R2, and H3T3 make large contributions, while Lys4 is not one of the major contributors, even though these modules are often referred to as *readers* of the unmodified H3K4.[9,47] Histone H3K4A substitution does not alter the binding affinity of KDM5B (K_d = 13 μM, Figure 3A, B) from that of the wild type H3 peptide. Even though H3K4 has been shown to form a salt bridge with Asp308,[9] we observed little change in affinity upon its substitution. This may also suggest other possible modes of contribution of Asp308 rather than its

DOI: 10.1021/acs.biochem.5b00617
Biochemistry 2015, 54, 5766−5780

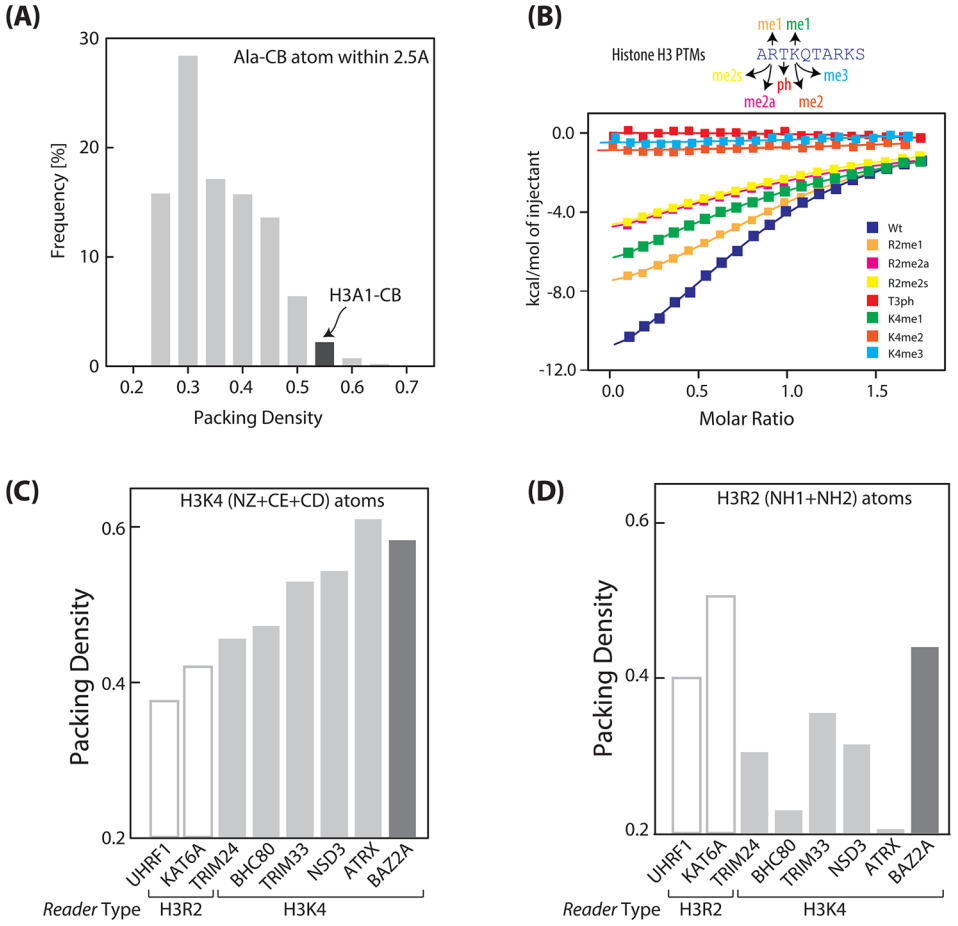

Figure 4. Interfacial packing and PTMs: (A) Distribution of packing density of Ala-CH_3 in proteins within the shell of 2.5 Å from the protein surface. The packing density of the H3Ala1-CH_3 group is in the dark gray bar. (B) ITC peptide binding titration profiles of KDM5B-PHD1 with H3 peptides bearing site-specific modifications. (C) Average packing density of H3K4 (NZ + CE + CD) atoms in different unmodified histone H3 *reader*-peptide complexes. White and gray bars, respectively, are for H3R2 and H3K4 *readers.* The light gray bars represent *readers* where H3K4 is engaged in salt bridge(s). (D) Average packing density of H3R2 (NH1 + NH2) atoms. White and gray bars, respectively, are for H3R2 and H3K4 *readers*..

taking part only in forming the salt bridge with H3K4. For example, Asp308 may provide a general electrostatic environment for the positively charged peptide. Similarly, for BAZ2A-PHD, the drop in affinity upon substitution of H3K4 with Ala is also small (Figure 3B). As mentioned above, the H3K4 residue in the BAZ2A-PHD-H3 complex does not participate in any salt bridge and is hydrogen bonded to the protein backbone. In the case of AIRE-PHD1, however, substitution of H3K4 by Ala disrupts a key salt bridge and thus completely abolishes peptide binding. Hence, it is tempting to argue that the H3K4 salt bridge is responsible for the large energetic contribution to the H3K4 residue and that the absence of a salt bridge results in a small energetic contribution. In other words, the observed trend of energetics may not rule out the possibility of an H3K4 residue being engaged with a backbone hydrogen bond in the KDM5B-PHD1 complex in place of the reported salt bridge. For AIRE-PHD1, the energetic contributions of peptide residues also have other differences from the other two PHD fingers. For AIRE-PHD1, almost all of the histone residues make energetic contributions, with six residues contributing ~1.0 kcal/mol. In other words, domains belonging to the same fold, even when binding to the same region of the peptide, do not necessarily utilize the exact same mechanism for peptide anchoring. The behavior of KDM5B-PHD1 and BAZ2A-PHD are closer to each other than to AIRE-PHD1. KDM5B-PHD1 and BAZ2A-PHD not only have a treble clef Asp pair feature but also respond to histone peptide mutations in a similar fashion. Hence, it is tempting to suggest that the treble clef Asp-pair feature represents a PHD subtype that includes the H3R2 *readers* and that these differ from typical H3K4 *readers* in terms of binding energetics. The loss of binding due to Arg residue substitution also suggests that deimination of Arg to citrulline could affect the ionic interactions and thus the anchoring of these PHD fingers. Peptidylarginine deiminase 4 (PADI4), a corepressor that deiminates Arg residues of nuclear proteins yielding citrulline,[48,49] could thus play an additional role in finely regulating the action of these proteins.

KDM5B is known to colocalize with histone H3K4me3 (an activation mark) in embryonic stem cells, especially at the promoters of the core pluripotency regulators *Oct4* (also known as *Pou5f1*), *Sox2*, and *Nanog*.[12] H3K4me3 is the substrate for the KDM5B JmjC demethylase enzyme module, and hence, the observed colocalization is consistent with the KDM5B JmjC demethylase function. Interestingly, 83% of H3K4me3 marks, including H3K4me3 and H3K27me3 (a repressive mark), with which KDM5B colocalizes in ES cells are bivalent marks.[12] Given the importance of PHD1 in demethylase activity,[16] it is intriguing what KDM5B-PHD1 would contribute to these sites, as it binds to the peptide without any methylation. Is it possible that the unmodified

DOI: 10.1021/acs.biochem.5b00617
Biochemistry 2015, 54, 5766−5780

H3K4me0 mark (a repressive mark) is also present within the bivalent marks and contributes to the localization of KDM5B? The answer to this question in ES cells will need to be probed by chromatin immunoprecipitation sequencing (ChIP-Seq). As we note here, the H3R8 residue also has a substantial contribution to the interaction with KDM5B-PHD1, and the histone peptide interaction likely extends for up to 8−9 residues. This extended H3 peptide interaction with KDM5B-PHD1 could also serve well for the specificity needed for ChIP-Seq reagents, and KDM5B-PHD1 may be utilized to probe genome-wide H3K4me0 marks, given the recent success in utilizing highly specific histone peptide-interacting modules[17] for this purpose.

The propensity ratio (*Fr_e*/*Fr_b*, see Methods) of peptide hot spot residues (in decreasing order) is W, F, Y, L, and I.[20] As histone peptides lack these amino acids, we wanted to learn the strategies that proteins utilize for binding to peptide sequences rich in Arg/Lys. We computed residue propensity ratio (*Fr_e*/*Fr_b*) for sequences rich in Arg/Lys in the nonredundant high-resolution peptide−protein complex structural data set (see Methods). For peptide sequences having at least one Arg residue, the preferred hot spot residues are W, F, I, L, Y, and R, where *Fr_e*/*Fr_b* for I, L, Y, and R were all close to ∼1.4. However, for sequences with at least one Lys residue, *Fr_e*/*Fr_b* for Lys was still <1.0. In other words, a peptide Arg residue when present at the binding site has a higher chance of being a hot spot than does Lys. KDM5B-PHD1 and BAZ2A-PHD seem to exploit the presence of histone Arg residues, and, as stated above, it is interesting to note that ancient homologues of KDM5B-PHD1 retained the histone peptide Arg-interacting residues, while Lys-interacting residues are a recent addition (Figure 1).

Interfacial Packing. Peptide−protein interfaces have been noted as being very tightly packed, even more tightly packed than protein−protein interfaces.[20] The loss of methyl groups in large-to-small nonpolar amino acid substitutions in well-packed protein interiors have been observed to result in a loss of ∼1 kcal.mol^{-1} of free energy.[50] The drop in affinity due to H3A1G substitution for all three PHD fingers (Figure 3) examined here is indicative of a substantial loss in packing at the H3-binding interface of PHD fingers. The packing density (see Methods) of atoms varies depending on their distance from the surface.[51] The packing density of the methyl group of Ala residues, in our calculations, is ∼0.36 in the shell within 2.5 Å of the surface and ∼0.56 for positions deeper than 2.5 Å from the surface (Figure S2A). We computed the packing density for the methyl group of the H3A1 residue in 14 high-resolution X-ray structures (≤2.0 Å, Figure S2B) of all PHD fingers in complex with either the modified or the unmodified histone H3 peptides. In all complexes, the distance of the H3A1-CH_3 group from the surface (average distance 2.29 ± 0.40 Å) is within the 2.5 Å, while it is packed with a much higher packing density (0.55 ± 0.05, Figure 4A, left), suggesting a highly packed environment for the H3A1-CH_3 group. Residues at three regions in the PHD fingers make contact with the H3A1-CH_3 group (Figure S2B). The first of these positions contains L/I/V, the second one usually a P, and the last one always W/Y (Figure S2B). These positions are highly conserved in the PHD finger family (Figure S2B), which suggests that tight packing of H3A1-CH_3 groups is likely to be a feature common to all PHD finger complexes irrespective of the subtypes, not just in the three PHD fingers studied here.

We also wanted to check the role of packing to better understand how the introduction of bulky functional groups of post-translational modifications (PTMs) disrupts peptide−protein interfaces. In particular, we focused on the packing density of NZ + CE + CD atoms of Lys residues for the effect of the introduction of methyl groups into H3K4 for *readers* of the unmodified histone H3 N-terminus. Ninety-five percent of Lys4 NZ + CE + CD atoms are observed within 2.5 Å from the surface, and their packing densities range from 0.2−0.7 (Figure S2C). How are the packing densities of H3 Lys4 NZ + CE + CD atoms distributed in the high-resolution X-ray structures (≤2.0 Å, Figure 4C) of seven PHD finger *readers* in complex with the unmodified histone H3 N-terminus? The H3 Lys4 NZ + CE + CD atoms in these complexes are within 2.5 Å of the surface, and their packing densities are in the range 0.35−0.6. For the UHRF1−peptide complex, the H3 Lys4 NZ + CE + CD atoms have a lower packing density, while the packing density increases when the H3K4-NZ atom is engaged in a salt bridge (Figure 4C). The packing density is observed to be the highest for ATRX, where the H3K4-NZ atom is engaged with two salt bridges.[52,53] UHRF1 and KAT6A PHD fingers are H3R2 *readers*,[43,44] and the effect of H3K4 methylation on the disruption of these peptide−protein complexes is small. The UHRF1 complex is not disrupted by H3K4 methylation,[43] while the interaction is weakened for KAT6A-PHD.[44] The low packing density of H3 Lys4 NZ + CE + CD atoms is likely less of a hindrance in accommodating the methyl groups. By contrast, for TRIM24, BHC80, TRIM33, NSD3, and ATRX PHD fingers, peptide binding is severely compromised by H3K4 methylation.[52,54−56] It is tempting to argue that the introduction of methyl groups on the NZ atom interferes with the salt bridge(s) in these complexes, leading to binding disruption. The example of BAZ2A, with a high packing density of H3 Lys4 NZ + CE + CD atoms (Figure 4C), emphasizes the role of tight packing. Despite the histone Lys4 residue not being involved in forming the salt bridge in BAZ2A,[47] the complex can respond to methylation due to tight packing. AIRE-PHD1 belongs to the group of proteins with salt bridge-dependent anchoring of H3K4 residues similar to that of H3K4 complexes with TRIM24, BHC80, TRIM33, NDS3, and ATRX. In this group, we observed a large energetic contribution of the H3K4 residue (Figure 3) as well as binding disruption upon H3K4 methylation. However, we note that the BAZ2A[47] and KDM5B complexes (Figure 4B, KDM5B) are disrupted by H3K4 methylation, even when H3K4 has a small energetic contribution. The commonality between these cases is that H3 Lys4 NZ + CE + CD atoms are likely to be tightly packed to respond to Lys methylation in a similar way.

Effect of PTMs on Peptide Binding. In addition to the observed behavior of H3K4 methylation on the formation of the KDM5B-PHD1−histone peptide complex, we have also looked at modifications at other peptide positions (Figure 4B) to determine whether they are consistent with those reported in the previous structural study.[9] Peptide binding is compromised upon methylation of the Arg2 residue, and the binding affinity is progressively reduced when comparing mono- to dimethylation, as expected with an increase in the size of the functional group (Figure 4B) at a packed interface. The packing density of the H3Arg2 side chain NH1 + NH2 atoms (Figure 4D) in the above complexes shows that the H3R2 *readers* (KAT6A and UHRF1) are packed more tightly than the H3K4 *readers*. In the ATRX and BHC80 complexes, the NH1 + NH2 atoms of the H3R2 residue show a very low packing density, and these

DOI: 10.1021/acs.biochem.5b00617
Biochemistry 2015, 54, 5766−5780

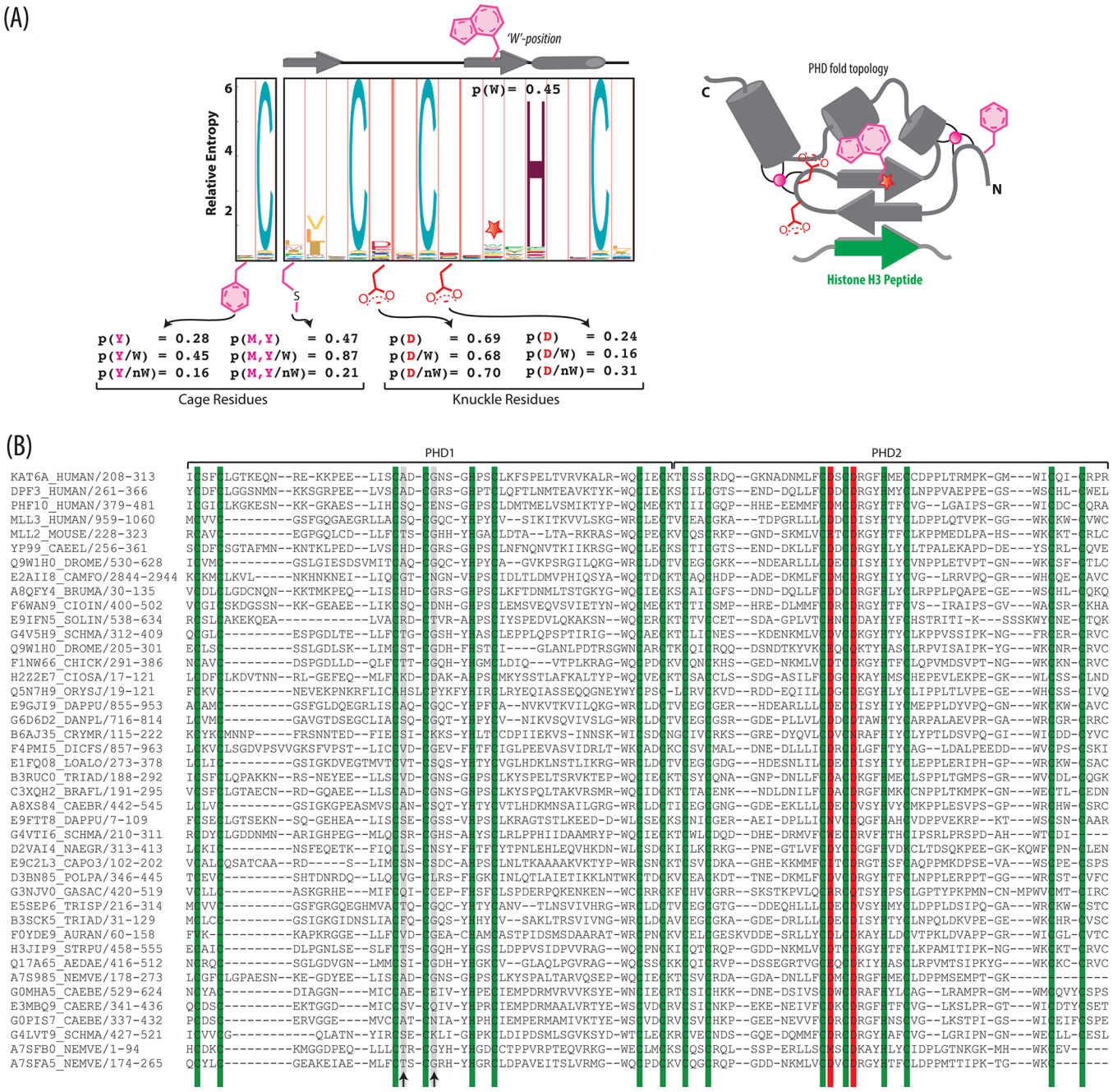

Figure 5. PHD subtypes and residue occurrence frequency: (A) sequence logo showing a portion of the PHD finger family with the secondary structural elements on top. The red star represents the *W-position*. The dependency of occurrence frequency of residues at specific positions is shown below the logo, and this is represented as probability and conditional probability (see text). The condition here is the presence or absence of W/F/Y at the *W-position*. Some of these positions are shown in the PHD topology (right) for convenience. (B) Alignment of tandem PHD−PHD sequences. Each sequence in the alignment is from a cluster of sequences where every member has more than 75% sequence identity with others. Red and gray bars, respectively, show the presence and absence of Asp residues, and the Zn chelating positions are in green.

complexes are less likely to be affected by H3R2 methylation. This is consistent with the recent report showing minimal effect on the ATRX-H3 peptide complex upon H3R2 methylation.[57] By contrast, for the complexes involving other *readers*, the values are in the intermediate range. In the BAZ2A−histone peptide complex, however, the NH1 + NH2 atoms of the H3R2 residues are packed as well as those of the H3R2−*reader* (KAT6A and UHRF1) complexes. It is tempting to suggest that electrostatic interactions between the H3R2 residue and the pair of Asp residues in the treble clef knuckle, a common feature in BAZ2A, KAT6A, and UHRF1 proteins, result in tighter packing of the H3R2 residues. For the observed effect of H3R2 methylation (Figure 4B) and the presence of Asp residues in the treble clef knuckle, we expect the H3R2 residue in a complex with KDM5B-PHD1 to be packed in a manner similar to that in complexes with BAZ2A, KAT6A, and UHRF1. The weakened interactions upon H3R2 methylation may weaken the anchoring of KDM4B-PHD1 onto chromatin, which suggests that the H3R2-specific methylases protein arginine *N*-methyltransferase 4 (PRMT4) and protein arginine *N*-methyltransferase 6 (PRMT6) could play a regulatory role in the localization of KDM5B on the chromatin. Phosphorylation

DOI: 10.1021/acs.biochem.5b00617
Biochemistry 2015, 54, 5766−5780

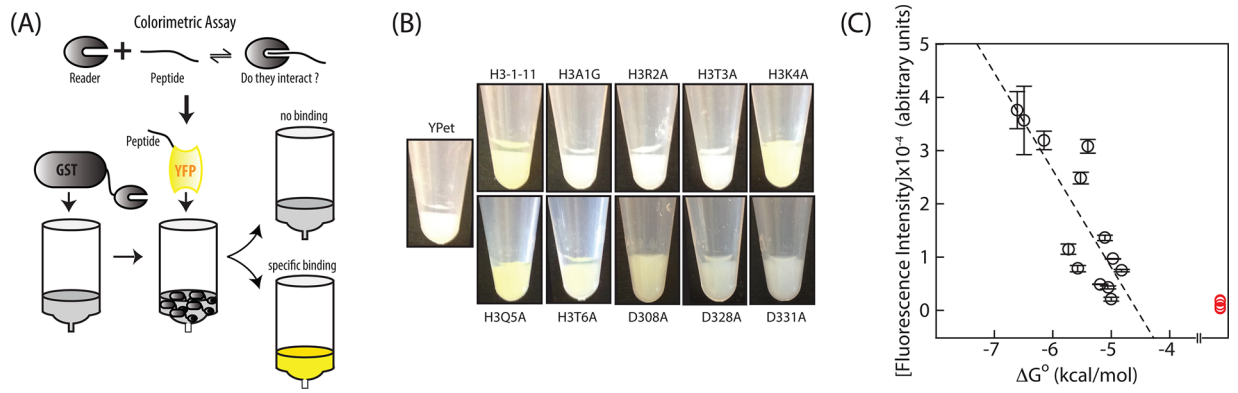

Figure 6. Colorimetric assay: (A) Colorimetric binding assay scheme. (B) Color gradient for the various mutants of H3 and hKDM5B-PHD1. (C) Relationship between the bead fluorescence and ΔG° of the interactions obtained from ITC. hKDM5B- and hAIRE-PHD1 interactions are used in this plot. Red circles represent those interactions where binding was not detected by ITC.

of Thr3 also completely aborts peptide binding (Figure 4B). The interface-disruptive nature of Lys4 methylation and Thr3 phosphorylation also suggest that methylases (Trx/Set1, PRDM9, MLL, and ASH1) specific for H3K4 and a kinase (Haspin) specific for H3T3 could play an important regulatory role in the anchoring of KDM5B onto chromatin. These binding studies suggest possible roles for a number of enzymes that could influence KDM5B localization and provide an opportunity to verify these speculations with detailed experimentation. These binding results are also very useful for comparing the binding behavior of paralogues (*see below*) and orthologues.

PHD Finger Subtypes and Position-Specific Residue Preferences. The PHD finger family shows subtype-specific amino acid preferences at specific sequence positions (Figures 5A and S3). For example, one notes the presence of an aromatic residue, predominantly Trp, in the second β-strand (the *W-position*, Figures 5A and S3) in the subtype that recognizes H3K4me3. Subtypes that bind unmodified histone H3 lack the second β-strand Trp but instead have different patterns of Asp residues at distinct positions (Figure S3). These observations suggest sequence-based predictability of PHD-binding subtypes, and we wanted to understand how useful a descriptor such as the presence of a position-specific amino acid would be as a subtype classifier. Having noted the presence of two Asp residues, a distinct feature in the treble clef knuckle of the H3R2 *reader* subtype (UHRF1 and KAT6A in Figure S3), we wanted to probe the behavioral characteristics of sequences that share the same feature (e.g., KDM5B and BAZ2A). It is encouraging to observe that for both KDM5B and BAZ2A PHD finger complexes, the absence of an H3 Lys4 residue did not significantly affect peptide binding, while the H3 Arg2 residue made large energetic contributions. Not needing a large energetic contribution from the H3 Lys4 residue for peptide binding could be a feature defining potential H3R2 subtypes but will need to be experimentally verified with a larger set of sequences. The sequence feature of the Asp residue (xC**D**xC**D**x) pair in the PHD finger treble clef is further analyzed in the next section.

For convenience of the discussion here, we group the PHD sequences into two major sets: (i) PHD_W, sequences with a Trp residue at the *W- position* and (ii) PHD_nW, sequences, without a Trp residue at the *W-position*. We justify this grouping based on our observation that residue positions that form the cage with the *W-position* (for enclosing H3K4me3) are enriched with cage-forming residues in the PHD_W set (Figure 5A), while the frequency of cage residues at these positions drops in the PHD_nW set (Figure 5A). For example, the frequency of Y, the first cage-forming residue in the entire PHD family is 0.28, while the frequency rises to 0.45 in the PHD_W set and drops to 0.16 in the PHD_nW set (Figure 5A). Similarly, the frequency of the cage-forming Met residue also shows a subtype-specific dependency (Figure 5A). This suggests that residue preferences are correlated with subtype and that subtype grouping by this criterion is reasonable. PHD_W and PHD_nW constitute ∼45% and ∼55% of PHD sequences, respectively. One would expect ∼45% of PHD family members to be H3K4me3 *readers*, while in the remaining 55% of the family, some may bind unmodified histones (H3K4 and H3R2) or may not bind peptides at all using the canonical peptide binding site. The occurrence frequency of the first Asp residue in the xC**D**xCxx knuckle in the PHD family is 0.70 (Figure 5A). This frequency remains the same in both the PHD_W and PHD_nW groups. The Asp at this position is likely to play an equally important role in both groups for its interaction with the H3R2 residue. The occurrence frequency of the second Asp residue in the xCxxCDx treble clef knuckle in the family is 0.24. However, the frequencies of the second Asp in the PHD_nW and PHD_W sequence groups are, respectively, 0.31 and 0.16, suggesting a group-specific preference for Asp, similar in pattern to that seen for cage-forming residues. The drop from the PHD_nW group to the PHD_W group (0.31 to 0.16) suggests that an additional electrostatic interaction with the H3R2 residue is preferred in the PHD_nW group. This could be due to the fact that the bulk of the binding energy in the H3K4me3 subtype depends on the methylated Lys residue and that the energetic contribution of H3 Arg2 can be small. However, in the PHD_nW group, the H3 Arg2 contribution is expected to be large, and the presence of additional Asp residues likely strengthens the interaction. The frequencies of the xC**D**xC**D**x Asp pair in the entire family and in the subtypes PHD_nW and PHD_W are, respectively, 0.21, 0.28, and 0.10; therefore, a sizable fraction (28%) of the PHD_nW group carries the xC**D**xC**D**x sequence feature, and this subtype may interact with unmodified histone H3.

PHD fingers also appear in tandem, namely, as PHD−PHD proteins. The frequency of the treble clef Asp residues in the tandem PHD−PHD protein strikingly differs (Figure 5B) from that observed above for single-PHD fingers. For PHD1 in the

DOI: 10.1021/acs.biochem.5b00617
Biochemistry 2015, 54, 5766−5780

tandem PHD−PHD protein, the Asp residues are completely absent from both positions of the treble clef. Interestingly, for PHD2 in the tandem PHD−PHD protein, Asp residues are almost always present at both treble clef knuckle positions (Figure 5B). Neither PHD1 nor PHD2 in the tandem PHD−PHD protein retains a Trp residue in the *W-position* and are unlikely to bind H3K4me3. Human KAT6A and DPF3 are well-known tandem PHD−PHD members who utilize the canonical binding site of PHD2 to accommodate an unmodified N-terminal H3 peptide but also utilize a distant site for anchoring peptide C-terminal acetylated Lys residues.[44,58] A majority of the positions characteristic of the PHD family are retained in the PHD1 and PHD2 fingers of the tandem PHD−PHD protein, yet the treble clef knuckle Asp residues remain a characteristic feature of all tandem PHDs (even among diverse sequences), and many of them are likely to bind unmodified histone H3.

Colorimetric Binding Assay. In this assay, a *reader*, recombinantly fused to GST or the His-tag, is immobilized on beads, and the fluorophore-tagged peptide of interest is then passed through the beads to check for retention of color (Figure 6A; see Methods). This approach is similar to the estimation of protein−protein-interaction affinity by quantifying bead-associated fluorescence using flow cytometry,[59,60] in which a protein immobilized on polystyrene beads is probed with a fluorescently labeled binding partner. In place of flow cytometry, we monitored the bead-associated fluorescence using a plate reader. Bead-associated fluorescence was compared with the ΔG° obtained using ITC (Figure 6C). The relationship between the amount of the complex retained in the beads and the ΔG° (or pK_d or $-\log(K_d)$) of the interaction is sigmoidal (Figure S4), in which intermediate affinities fall on the transition region of the sigmoidal curve, while extremely high and low affinities fall in the two baseline regions. Mutants for which we do not observe any binding in the ITC titrations show a very low level of fluorescence (Figure 6C, red circles), indicating extremely low affinity, while intermediate affinities show a linear relationship, suggesting consistency between the two different methods. We utilized this approach to rapidly measure the histone-binding tendencies of paralogues and close sequence homologues (see below). This approach resembles the classical GST pull-down[61] assay that has been extensively used for measuring histone peptide binding as well as protein−protein interactions in general. Our assay does not require SDS−PAGE or Western blotting following the pull-down steps, yet it provides a rapid visual assessment of binding, adding to convenience. Peptide-based dot blot array methods[62−64] are also elegant and used widely but also depend on antibody-based Western blot-like assessment. The recombinant peptide-fused fluorescent proteins can be produced in large quantities, are stable, can be stored frozen, and can be reused upon thawing without loss of activity. This method complements other methods and, as a general application, can be used to rapidly determine the effect of point mutations on protein−protein interactions for proteins for which arrays are unavailable.

Peptide-Binding Behavior of hKDM5B-PHD1 Paralogues and Other Homologues. In the PHD family, it was noted earlier that there can be sequences with as little as ∼20% identical residues that yet bind the same peptide as long as the key peptide-anchoring residues are retained.[65] Hence, we wanted to determine whether the presence of the treble clef knuckle Asp pair would be sufficient for unmodified histone H3 binding. Besides, there are several examples of non-PHD protein modules that anchor the peptide Arg residue by the Asp/Glu residue pair, in which the peptide Arg makes a large energetic contribution (Figure S5). Several human PHD fingers have this feature, such as the first PHD finger of human KDM5B paralogues (KDM5A, KDM5C, and KDMD), PHD fingers of human RSF1 and PHRF1 (Figure S6A), and tandem PHD−PHD fingers of human MLL2, MLL3, PHF10, REQU, A5PLL3, and other proteins. Using the colorimetric assay discussed above, we determined whether human RSF1-PHD and KDM5D-PHD1 bind unmodified histone H3 peptide. These two proteins, however, do not show any detectable binding (Figure S6B), even though they share >20% identical residues with KDM5B-PHD1. KDM5B- and KDM5D-PHD1 share ∼60% identical residues, including the pair of Asp residues, but only one interacts with the histone peptide. The structure of KDM5D-PHD1 (PDB ID 2e6r) is analyzed further (see Methods for details) as the structure does not show any major structural deviation (Figure S7A) from other members of the family. When placing an artificial peptide onto the KDM5D-PHD1 binding site, we observed that the hydrogen bond between the peptide terminal NH_3^+ group and KDM5D-PHD1 is constrained (Figure S7B, bottom): specifically, 30% of the hydrogen bond lengths are less than 2.0 Å. While repeating the peptide-swapping experiment with positive controls (see Methods), a much smaller percentage of the terminal hydrogen bonds are <2.0 Å (Figure S7B,, bottom). Although a crude measure, this points to subtle differences that may exist between closely related sequences such as paralogues.

Differences in peptide-binding behavior between PHD finger paralogues have also been reported previously (Figure S6C): for example, NSD3-PHD5 and NSD1-PHD5.[56] A number of similar example pairs with high sequence identity, where one binds and other does not, are discussed further in Figure S6. The non-PHD protein pair of Ago3 and Ago2 is also noteworthy for striking differences in their RNA slicing behavior, despite identical functional residues at the catalytic site.[66,67] In other words, factors in addition to the presence of key residues may determine the overall function of proteins belonging to the same fold. Like the Ago2 and Ago3 study,[66,67] these observations suggest that a systematic mutagenesis study will be needed to identify the true signature for peptide binding in a superfamily. On the basis of the earlier report of the dependency of KDM5B demethylase activity on PHD1,[16] the peptide-binding observations provide an opportunity to probe whether the differences in KDM5B and KDM5D demethylase activity as well as their localization are linked to the difference in the peptide-binding behavior of the first PHD finger.

■ CONCLUSIONS

Using ITC to capture the energetic contribution of residues, in this case study we learn that *readers* of the same fold even when binding the same peptide substrate may utilize very different recognition chemistry, and as a result can respond to post-translational modifications differently. Using explicit measure of packing density, we show that peptide−protein interfacial packing likely plays a very important regulatory role. Loss of tight packing (due to large to small amino acid substitution) as well as over packing (due to PTM functional groups) can result in a significant loss of binding. We interestingly also note that even if the energetic contribution of a tightly packed residue is small, introduction of PTM on that residue can still disrupt binding. With respect to peptide recognition features, on one

DOI: 10.1021/acs.biochem.5b00617
Biochemistry 2015, 54, 5766−5780

side we note that presence of a few characteristic residues can result in subtype specific behavior. While on the other side, we also note that proteins with very similar sequences, in spite of the presence of the key functional/characteristic residues, may not behave the same way. Subtle structural differences may result in striking functional differences. Hence, we provide a convenient fluorescent binding assay that can provide rapid assessment of binding behavior, and the approach can later be used for systematic studies to better understand the peptide binding behavior of large protein families. We also note that conservation of residues among orthologs can be useful to probe structural and functional role of amino acids. Overall, this study showcases histone interactions in the context of residue conservation, energetic contributions, interfacial packing, and sequence-based *reader* subtype predictability, and the lessons learned here would be useful for studying other large protein families as well as designing histone peptide specific binding reagents.

■ ASSOCIATED CONTENT

Supporting Information

The Supporting Information is available free of charge on the ACS Publications website at DOI: 10.1021/acs.biochem.5b00617.

Human KDM5B and ING4 PHD fingers; Asp residues and the PHD knuckle; peptide residue contributions; interfacial packing and PTMs; PHD subtypes and residue occurrence frequency; and the colorimetric assay (PDF)

■ AUTHOR INFORMATION

Corresponding Author

*Tel: 1-605-688-5694. Fax: +1-605-688-6364. E-mail: suvobrata.chakravarty@sdstate.edu.

Author Contributions

†C.S. and E.F. contributed equally, and are joint first authors.

Funding

This material is based upon work supported by the National Science Foundation/EPSCoR Award No. IIA-1355423 and by the state of South Dakota, through BioSNTR (Biochemical Spatiotemporal NeTwork Resource). The study was also supported by funds from BCAAP (Biological Control and Analysis by Applied Photonics, the South Dakota 2010 center grant), SDSU (South Dakota State University) Agricultural Experimentation Station, and SDSU Department of Chemistry & Biochemistry Startup Funds to S.C.

Notes

Any opinions, findings, and conclusions or recommendations expressed in this material are those of the author(s) and do not necessarily reflect the views of the National Science Foundation.

The authors declare no competing financial interest.

■ ACKNOWLEDGMENTS

We thank Adam Hoppe for the generous gift of the mCitrine construct, access to the plate reader, comments on the manuscript, and for all the encouragement. We thank John Robinson and Jason Kerkvliet for access to instrumentation for protein quantification, purification, and for help with the plate reader, respectively. S.C. thanks Gaetano T. Montelione and Ora Schueler-Furman for the discussions on NMR structure quality and peptide binding energetics, respectively. S.C. thanks Brian Moore for computational support. S.C. thanks Matt Miller for undergraduate student (S.Z.) participation in research through CHEM237.

■ ABBREVIATIONS

KDM5B, lysine (***K***) specific ***dem***ethylase 5B; PHD, ***p***lant ***h***omeo***d***omain; PTM, ***p***ost-***t***ranslational ***m***odification; BAZ2A, ***b***romodomain ***a***djacent to ***z***n-finger domain protein 2***A***; AIRE, ***a***uto***i***mmune ***re***gulator; UHRF1, ***u***biquitin-like P***H***D and ***R***ING ***f***inger domains 1; KAT6A, Lysine (***K***) ***a***cetyla***t***ransferase 6A; PRMT, ***p***rotein ***a***rginine ***m***ethyl***t***ransferase; PADI, ***p***eptidyl ***a***rginine ***d***eiminase; MLL2, ***m***ixed ***l***ineage ***l***eukemia 2; ASH1, ***a***djacent ***s***mall ***h***omeotic 1; GST, ***g***lutathione ***S***-***t***ransferase; IPTG, ***i***sopro***p***yl *β*-D-1-***t***hio***g***alactopyranoside; ITC, ***i***sothermal ***t***itration ***c***alorimetry; FPLC, ***f***ast ***p***rotein ***l***iquid ***c***hromatography; NMR, ***n***uclear ***m***agnetic ***r***esonance

■ REFERENCES

(1) Smith, E., and Shilatifard, A. (2010) The chromatin signaling pathway: diverse mechanisms of recruitment of histone-modifying enzymes and varied biological outcomes. *Mol. Cell 40*, 689−701.

(2) Schreiber, S. L., and Bernstein, B. E. (2002) Signaling network model of chromatin. *Cell 111*, 771−778.

(3) Pincus, D., Letunic, I., Bork, P., and Lim, W. A. (2008) Evolution of the phospho-tyrosine signaling machinery in premetazoan lineages. *Proc. Natl. Acad. Sci. U. S. A. 105*, 9680−9684.

(4) Ruthenburg, A. J., Allis, C. D., and Wysocka, J. (2007) Methylation of lysine 4 on histone H3: intricacy of writing and reading a single epigenetic mark. *Mol. Cell 25*, 15−30.

(5) Seet, B. T., Dikic, I., Zhou, M. M., and Pawson, T. (2006) Reading protein modifications with interaction domains. *Nat. Rev. Mol. Cell Biol. 7*, 473−483.

(6) Patel, D. J., and Wang, Z. (2013) Readout of epigenetic modifications. *Annu. Rev. Biochem. 82*, 81−118.

(7) Musselman, C. A., Lalonde, M. E., Cote, J., and Kutateladze, T. G. (2012) Perceiving the epigenetic landscape through histone readers. *Nat. Struct. Mol. Biol. 19*, 1218−1227.

(8) Klein, B. J., Piao, L., Xi, Y., Rincon-Arano, H., Rothbart, S. B., Peng, D., Wen, H., Larson, C., Zhang, X., Zheng, X., Cortazar, M. A., Pena, P. V., Mangan, A., Bentley, D. L., Strahl, B. D., Groudine, M., Li, W., Shi, X., and Kutateladze, T. G. (2014) The histone-H3K4-specific demethylase KDM5B binds to its substrate and product through distinct PHD fingers. *Cell Rep. 6*, 325−335.

(9) Zhang, Y., Yang, H., Guo, X., Rong, N., Song, Y., Xu, Y., Lan, W., Zhang, X., Liu, M., Xu, Y., and Cao, C. (2014) The PHD1 finger of KDM5B recognizes unmodified H3K4 during the demethylation of histone H3K4me2/3 by KDM5B. *Protein Cell 5*, 837−850.

(10) Zou, M. R., Cao, J., Liu, Z., Huh, S. J., Polyak, K., and Yan, Q. (2014) Histone demethylase jumonji AT-rich interactive domain 1B (JARID1B) controls mammary gland development by regulating key developmental and lineage specification genes. *J. Biol. Chem. 289*, 17620−17633.

(11) Li, X., Liu, L., Yang, S., Song, N., Zhou, X., Gao, J., Yu, N., Shan, L., Wang, Q., Liang, J., Xuan, C., Wang, Y., Shang, Y., and Shi, L. (2014) Histone demethylase KDM5B is a key regulator of genome stability. *Proc. Natl. Acad. Sci. U. S. A. 111*, 7096−7101.

(12) Kidder, B. L., Hu, G., and Zhao, K. (2014) KDM5B focuses H3K4 methylation near promoters and enhancers during embryonic stem cell self-renewal and differentiation. *Genome biology 15*, R32.

(13) Kano, Y., Konno, M., Ohta, K., Haraguchi, N., Nishikawa, S., Kagawa, Y., Hamabe, A., Hasegawa, S., Ogawa, H., Fukusumi, T., Noguchi, Y., Ozaki, M., Kudo, T., Sakai, D., Satoh, T., Ishii, M., Mizohata, E., Inoue, T., Mori, M., Doki, Y., and Ishii, H. (2013) Jumonji/Arid1b (Jarid1b) protein modulates human esophageal cancer cell growth. *Mol. Clin. Oncol. 1*, 753−757.

DOI: 10.1021/acs.biochem.5b00617
Biochemistry 2015, 54, 5766−5780

(14) Enkhbaatar, Z., Terashima, M., Oktyabri, D., Tange, S., Ishimura, A., Yano, S., and Suzuki, T. (2013) KDM5B histone demethylase controls epithelial-mesenchymal transition of cancer cells by regulating the expression of the microRNA-200 family. *Cell Cycle 12*, 2100−2112.
(15) Christensen, J., Agger, K., Cloos, P. A., Pasini, D., Rose, S., Sennels, L., Rappsilber, J., Hansen, K. H., Salcini, A. E., and Helin, K. (2007) RBP2 belongs to a family of demethylases, specific for tri-and dimethylated lysine 4 on histone 3. *Cell 128*, 1063−1076.
(16) Yamane, K., Tateishi, K., Klose, R. J., Fang, J., Fabrizio, L. A., Erdjument-Bromage, H., Taylor-Papadimitriou, J., Tempst, P., and Zhang, Y. (2007) PLU-1 is an H3K4 demethylase involved in transcriptional repression and breast cancer cell proliferation. *Mol. Cell 25*, 801−812.
(17) Kungulovski, G., Kycia, I., Tamas, R., Jurkowska, R. Z., Kudithipudi, S., Henry, C., Reinhardt, R., Labhart, P., and Jeltsch, A. (2014) Application of histone modification-specific interaction domains as an alternative to antibodies. *Genome Res. 24*, 1842−1853.
(18) Moore, K. E., Carlson, S. M., Camp, N. D., Cheung, P., James, R. G., Chua, K. F., Wolf-Yadlin, A., and Gozani, O. (2013) A general molecular affinity strategy for global detection and proteomic analysis of lysine methylation. *Mol. Cell 50*, 444−456.
(19) Kortemme, T., Kim, D. E., and Baker, D. (2004) Computational alanine scanning of protein-protein interfaces. *Sci. Signaling 2004*, pl2.
(20) London, N., Movshovitz-Attias, D., and Schueler-Furman, O. (2010) The structural basis of peptide-protein binding strategies. *Structure 18*, 188−199.
(21) Stein, A., Rueda, M., Panjkovich, A., Orozco, M., and Aloy, P. (2011) A systematic study of the energetics involved in structural changes upon association and connectivity in protein interaction networks. *Structure 19*, 881−889.
(22) Chen, J. R., Chang, B. H., Allen, J. E., Stiffler, M. A., and MacBeath, G. (2008) Predicting PDZ domain-peptide interactions from primary sequences. *Nat. Biotechnol. 26*, 1041−1045.
(23) Remaut, H., and Waksman, G. (2006) Protein-protein interaction through beta-strand addition. *Trends Biochem. Sci. 31*, 436−444.
(24) Chakravarty, S., Zeng, L., and Zhou, M. M. (2009) Structure and site-specific recognition of histone H3 by the PHD finger of human autoimmune regulator. *Structure 17*, 670−679.
(25) Pace, C. N., Vajdos, F., Fee, L., Grimsley, G., and Gray, T. (1995) How to measure and predict the molar absorption coefficient of a protein. *Protein Sci. 4*, 2411−2423.
(26) (2014) Activities at the Universal Protein Resource (UniProt), *Nucleic Acids Res. 42*, D191−D198.10.1093/nar/gkt1140
(27) Leinonen, R., Diez, F. G., Binns, D., Fleischmann, W., Lopez, R., and Apweiler, R. (2004) UniProt archive. *Bioinformatics 20*, 3236−3237.
(28) Ostlund, G., Schmitt, T., Forslund, K., Kostler, T., Messina, D. N., Roopra, S., Frings, O., and Sonnhammer, E. L. (2010) InParanoid 7: new algorithms and tools for eukaryotic orthology analysis. *Nucleic Acids Res. 38*, D196−203.
(29) Edgar, R. C. (2004) MUSCLE: multiple sequence alignment with high accuracy and high throughput. *Nucleic acids research 32*, 1792−1797.
(30) Punta, M., Coggill, P. C., Eberhardt, R. Y., Mistry, J., Tate, J., Boursnell, C., Pang, N., Forslund, K., Ceric, G., Clements, J., Heger, A., Holm, L., Sonnhammer, E. L., Eddy, S. R., Bateman, A., and Finn, R. D. (2012) The Pfam protein families database. *Nucleic Acids Res. 40*, D290−301.
(31) Li, W., Jaroszewski, L., and Godzik, A. (2002) Tolerating some redundancy significantly speeds up clustering of large protein databases. *Bioinformatics 18*, 77−82.
(32) Sali, A., and Blundell, T. L. (1993) Comparative protein modelling by satisfaction of spatial restraints. *J. Mol. Biol. 234*, 779−815.
(33) Shen, M. Y., and Sali, A. (2006) Statistical potential for assessment and prediction of protein structures. *Protein Sci. 15*, 2507−2524.
(34) Camacho, C. J., and Zhang, C. (2005) FastContact: rapid estimate of contact and binding free energies. *Bioinformatics 21*, 2534−2536.
(35) Champ, P. C., and Camacho, C. J. (2007) FastContact: a free energy scoring tool for protein-protein complex structures. *Nucleic Acids Res. 35*, W556−560.
(36) Rother, K., Hildebrand, P. W., Goede, A., Gruening, B., and Preissner, R. (2009) Voronoia: analyzing packing in protein structures. *Nucleic Acids Res. 37*, D393−395.
(37) Goede, A., Preissner, R., and Frommel, C. (1997) Voronoi Cell: new method for allocation of space among atoms: elimination of avoidable errors in calculation of atomic volume and density. *J. Comput. Chem. 18*, 1113−1123.
(38) Chakravarty, S., and Varadarajan, R. (1999) Residue depth: a novel parameter for the analysis of protein structure and stability. *Structure 7*, 723−732.
(39) Vanhee, P., Reumers, J., Stricher, F., Baeten, L., Serrano, L., Schymkowitz, J., and Rousseau, F. (2010) PepX: a structural database of non-redundant protein-peptide complexes. *Nucleic Acids Res. 38*, D545−551.
(40) McDonald, I. K., and Thornton, J. M. (1994) Satisfying hydrogen bonding potential in proteins. *J. Mol. Biol. 238*, 777−793.
(41) Sanchez, R., and Zhou, M. M. (2011) The PHD finger: a versatile epigenome reader. *Trends Biochem. Sci. 36*, 364−372.
(42) He, D., Fiz-Palacios, O., Fu, C. J., Fehling, J., Tsai, C. C., and Baldauf, S. L. (2014) An alternative root for the eukaryote tree of life. *Curr. Biol. 24*, 465−470.
(43) Rajakumara, E., Wang, Z., Ma, H., Hu, L., Chen, H., Lin, Y., Guo, R., Wu, F., Li, H., Lan, F., Shi, Y. G., Xu, Y., Patel, D. J., and Shi, Y. (2011) PHD finger recognition of unmodified histone H3R2 links UHRF1 to regulation of euchromatic gene expression. *Mol. Cell 43*, 275−284.
(44) Qiu, Y., Liu, L., Zhao, C., Han, C., Li, F., Zhang, J., Wang, Y., Li, G., Mei, Y., Wu, M., Wu, J., and Shi, Y. (2012) Combinatorial readout of unmodified H3R2 and acetylated H3K14 by the tandem PHD finger of MOZ reveals a regulatory mechanism for HOXA9 transcription. *Genes Dev. 26*, 1376−1391.
(45) Mao, B., Tejero, R., Baker, D., and Montelione, G. T. (2014) Protein NMR structures refined with Rosetta have higher accuracy relative to corresponding X-ray crystal structures. *J. Am. Chem. Soc. 136*, 1893−1906.
(46) Ramelot, T. A., Raman, S., Kuzin, A. P., Xiao, R., Ma, L. C., Acton, T. B., Hunt, J. F., Montelione, G. T., Baker, D., and Kennedy, M. A. (2009) Improving NMR protein structure quality by Rosetta refinement: a molecular replacement study. *Proteins: Struct., Funct., Genet. 75*, 147−167.
(47) Tallant, C., Valentini, E., Fedorov, O., Overvoorde, L., Ferguson, F. M., Filippakopoulos, P., Svergun, D. I., Knapp, S., and Ciulli, A. (2015) Molecular basis of histone tail recognition by human TIP5 PHD finger and bromodomain of the chromatin remodeling complex NoRC. *Structure 23*, 80−92.
(48) Wang, Y., Wysocka, J., Sayegh, J., Lee, Y. H., Perlin, J. R., Leonelli, L., Sonbuchner, L. S., McDonald, C. H., Cook, R. G., Dou, Y., Roeder, R. G., Clarke, S., Stallcup, M. R., Allis, C. D., and Coonrod, S. A. (2004) Human PAD4 regulates histone arginine methylation levels via demethylimination. *Science 306*, 279−283.
(49) Cuthbert, G. L., Daujat, S., Snowden, A. W., Erdjument-Bromage, H., Hagiwara, T., Yamada, M., Schneider, R., Gregory, P. D., Tempst, P., Bannister, A. J., and Kouzarides, T. (2004) Histone deimination antagonizes arginine methylation. *Cell 118*, 545−553.
(50) Chakravarty, S., Bhinge, A., and Varadarajan, R. (2002) A procedure for detection and quantitation of cavity volumes proteins. Application to measure the strength of the hydrophobic driving force in protein folding. *J. Biol. Chem. 277*, 31345−31353.
(51) Rother, K., Preissner, R., Goede, A., and Frommel, C. (2003) Inhomogeneous molecular density: reference packing densities and distribution of cavities within proteins. *Bioinformatics 19*, 2112−2121.
(52) Iwase, S., Xiang, B., Ghosh, S., Ren, T., Lewis, P. W., Cochrane, J. C., Allis, C. D., Picketts, D. J., Patel, D. J., Li, H., and Shi, Y. (2011)

DOI: 10.1021/acs.biochem.5b00617
Biochemistry 2015, 54, 5766−5780

ATRX ADD domain links an atypical histone methylation recognition mechanism to human mental-retardation syndrome. *Nat. Struct. Mol. Biol. 18*, 769−776.
(53) Eustermann, S., Yang, J. C., Law, M. J., Amos, R., Chapman, L. M., Jelinska, C., Garrick, D., Clynes, D., Gibbons, R. J., Rhodes, D., Higgs, D. R., and Neuhaus, D. (2011) Combinatorial readout of histone H3 modifications specifies localization of ATRX to heterochromatin. *Nat. Struct. Mol. Biol. 18*, 777−782.
(54) Tsai, W. W., Wang, Z., Yiu, T. T., Akdemir, K. C., Xia, W., Winter, S., Tsai, C. Y., Shi, X., Schwarzer, D., Plunkett, W., Aronow, B., Gozani, O., Fischle, W., Hung, M. C., Patel, D. J., and Barton, M. C. (2010) TRIM24 links a non-canonical histone signature to breast cancer. *Nature 468*, 927−932.
(55) Lan, F., Collins, R. E., De Cegli, R., Alpatov, R., Horton, J. R., Shi, X., Gozani, O., Cheng, X., and Shi, Y. (2007) Recognition of unmethylated histone H3 lysine 4 links BHC80 to LSD1-mediated gene repression. *Nature 448*, 718−722.
(56) He, C., Li, F., Zhang, J., Wu, J., and Shi, Y. (2013) The methyltransferase NSD3 has chromatin-binding motifs, PHD5-C5HCH, that are distinct from other NSD (nuclear receptor SET domain) family members in their histone H3 recognition. *J. Biol. Chem. 288*, 4692−4703.
(57) Noh, K. M., Maze, I., Zhao, D., Xiang, B., Wenderski, W., Lewis, P. W., Shen, L., Li, H., and Allis, C. D. (2015) ATRX tolerates activity-dependent histone H3 methyl/phos switching to maintain repetitive element silencing in neurons. *Proc. Natl. Acad. Sci. U. S. A. 112*, 6820−6827.
(58) Zeng, L., Zhang, Q., Li, S., Plotnikov, A. N., Walsh, M. J., and Zhou, M. M. (2010) Mechanism and regulation of acetylated histone binding by the tandem PHD finger of DPF3b. *Nature 466*, 258−262.
(59) Blazer, L. L., Roman, D. L., Muxlow, M. R., and Neubig, R. R. (2010) Use of Flow Cytometric Methods to Quantify Protein-Protein Interactions, *Current Protocols in Cytometry*, (Paul Robinson, J., et al., Eds.) Chapter 13, Unit 13, pp 11−15, Wiley, New York. 10.1002/0471142956.cy1311s51
(60) Nishikori, S., Hattori, T., Fuchs, S. M., Yasui, N., Wojcik, J., Koide, A., Strahl, B. D., and Koide, S. (2012) Broad ranges of affinity and specificity of anti-histone antibodies revealed by a quantitative peptide immunoprecipitation assay. *J. Mol. Biol. 424*, 391−399.
(61) Vikis, H. G., and Guan, K. L. (2004) Glutathione-S-transferase-fusion based assays for studying protein-protein interactions. *Methods Mol. Biol. 261*, 175−186.
(62) Nady, N., Min, J., Kareta, M. S., Chedin, F., and Arrowsmith, C. H. (2008) A SPOT on the chromatin landscape? Histone peptide arrays as a tool for epigenetic research. *Trends Biochem. Sci. 33*, 305−313.
(63) Bock, I., Kudithipudi, S., Tamas, R., Kungulovski, G., Dhayalan, A., and Jeltsch, A. (2011) Application of Celluspots peptide arrays for the analysis of the binding specificity of epigenetic reading domains to modified histone tails. *BMC[ ]Biochem. 12*, 48.
(64) Bua, D. J., Kuo, A. J., Cheung, P., Liu, C. L., Migliori, V., Espejo, A., Casadio, F., Bassi, C., Amati, B., Bedford, M. T., Guccione, E., and Gozani, O. (2009) Epigenome microarray platform for proteome-wide dissection of chromatin-signaling networks. *PLoS One 4*, e6789.
(65) Champagne, K. S., Saksouk, N., Pena, P. V., Johnson, K., Ullah, M., Yang, X. J., Cote, J., and Kutateladze, T. G. (2008) The crystal structure of the ING5 PHD finger in complex with an H3K4me3 histone peptide. *Proteins: Struct., Funct., Genet. 72*, 1371−1376.
(66) Hauptmann, J., Dueck, A., Harlander, S., Pfaff, J., Merkl, R., and Meister, G. (2013) Turning catalytically inactive human Argonaute proteins into active slicer enzymes. *Nat. Struct. Mol. Biol. 20*, 814−817.
(67) Schurmann, N., Trabuco, L. G., Bender, C., Russell, R. B., and Grimm, D. (2013) Molecular dissection of human Argonaute proteins by DNA shuffling. *Nat. Struct. Mol. Biol. 20*, 818−826.

DOI: 10.1021/acs.biochem.5b00617
Biochemistry 2015, 54, 5766−5780